Progress In Electromagnetics Research M, Vol. 77, 73–82, 2019

The Influence of the Terrain on Height Measurement Using the GNSS Interference Signal

Nan Zhang[1], Songhua Yan[1, *], Wenwei Wang[1], and Jianya Gong[2]

Abstract—Global Navigation Satellite System (GNSS) reflectometry is a promising technology used to estimate soil moisture, sea surface height, ice properties, etc. Interference signal technique is an important method to estimate these geophysical parameters. The effect of this method is closely related to the terrain and the receiving antenna placement. This study aims to investigate the effects of terrain and antenna placement on height measurement through simulation and field experiments. In this paper, we first simulated the interference signal in different types of terrain by parabolic equation method and analyzed the influence of terrain on the height measurement. Then we conducted three typical field experiments and processed experimental data. The simulated and experimental results indicate that the interference signal is affected by the terrain and the receiving antenna placement. Height measurement result is correct by both horizontal-looking and zenith-looking antenna when the ground is flat. However when the ground is not flat, the soil block near the receiving antenna leads to estimation errors. A more accurate estimation is obtained by using zenith-looking antenna to suppress the influence from the near terrain than horizontal-looking antenna. When a slope is near the receiving antenna, the signal with a high elevation may achieve an obvious interference effect if high elevation minus slope is equivalent to a low elevation. In this situation, the measurement height is the distance between the antenna and slope surface.

1. INTRODUCTION

Global Navigation Satellite System (GNSS) reflectometry is an emerging area of navigation satellite applications in the field of microwave remote sensing, where GNSS signals reflected from the earth are used as observation signals. GNSS reflectometry instrument has been placed on the satellites, airplanes and the ground for estimating soil moisture, sea surface height and ice properties [1–3]. In the ground-based experiment, the interference signal combined by the direct and reflected signals plays an important role. Its frequency provides the information of the antenna height and then can be used to estimate soil moisture or vegetation height [4, 5]. In order to improve the effect of the interference between the direct and reflected signal, sometimes the microstrip antenna was placed facing the horizontal direction so that the antenna has more gain to amplify the reflected signal [6, 7].

However, the desired effect of interference cannot be achieved in all terrains. It depends on antenna placement and ground topography. More detailed investigations are necessary for different types of terrain. In this study, we attempt to investigate the influence of the terrain and the antenna placement on the reflected GNSS signals through ground-based experiment.

The rest of this paper is organized as follows. Section 2 introduces GNSS interference technique for height measurement. Section 3 describes the parabolic equation method for low elevation grazing incidence signal as well as provides simulation results for different types of terrain. Section 4 provides

Received 14 October 2018, Accepted 8 December 2018, Scheduled 21 December 2018

* Corresponding author: Songhua Yan (ysh@whu.edu.cn).

[1] School of Electronic Information, Wuhan University, Wuhan, China. [2] School of Remote Sensing and Information Engineering, Wuhan University, Wuhan, China.

data processing steps and three field experiments focused on interference signal from different types of terrain including water surface, ground with soil block and slop surface. Section 5 presents the conclusions.

2. GNSS INTERFERENCE TECHNIQUE FOR HEIGHT MEASUREMENT

The received GNSS signal from a flat ground (ignoring the receiver antenna gain pattern) can be written as:

$$S = e^{j\phi} + \sum_{1}^{m} \rho_i e^{j(\phi+\psi_i)} \tag{1}$$

where m is the number of reflected signals, i the serial number of i-th multipath signal, ρ_i the magnitude of the reflection coefficient, ψ_i the total phase delay due to the reflection, and ϕ the phase of the direct signal.

It is proved in many studies that the received GNSS signal S is interference signal which is the composite signal caused by direct and reflected signals [8]. The interference signal is observed using signal-to-noise ratio (SNR) data output from receiver, changing with the elevation angle of the GNSS satellites at relatively low elevation. The interference signal manifests a quasi-periodic oscillating pattern created by the phase offset between direct and reflected signals. After filtering and detrending, a mathematical model for received GNSS signal S is obtained as:

$$S = |u_{dir}(\theta)|^2 + |u_{ref}(-\theta)|^2 + |A(\theta)| \cos\left[\frac{4\pi H}{\lambda}\sin\theta + \Psi\right] \tag{2}$$

where u, A are amplitude; θ is the elevation; λ is the wavelength; phase Ψ is independent of elevation θ but is related to soil moisture; and H is the distance between reflective surface and antenna. To simplify, the received GNSS signal S can be modeled as a three-parameter model $S = a\cos[2\pi f x + \Psi] + c$, where $x = \sin\theta$, $a = |A(\theta)|$, $c = |u_{dir}(\theta)|^2 + |u_{ref}(-\theta)|^2$ and $f = 2H/\lambda$. So f is the frequency of received GNSS signal and can be used to estimate the antenna height H.

However, when the ground surface is not flat, such as a raised soil block on the ground, the antenna height cannot be estimated correctly. In this research, we used the parabolic Equation (PE)-based microwave propagation model to simulate the ground-reflected multipath propagation behavior of GNSS signals, and then conducted three typical experiments of estimating the antenna height to investigate the effect of terrain on interference signal.

3. THE PARABOLIC EQUATION SIMULATION

3.1. Parabolic Equation Method

To investigate the influence of the terrain on the interference GNSS signals, PE method is employed. PE method is an approximation of the wave equation which models energy propagation in a cone centred on a preferred direction, where the absorbing boundary conditions is placed on the top and bottom of the computational area. This method allows for the large electrical domain sizes required for the analysis and takes into account the terrain factors, thus it is suitable for radio propagation analysis in the case of the incoming GNSS radio wave with a low elevation.

Here we give a short description of the principle of the PE method, and the details can be referred to [9] and [10]. The propagation model of GNSS signals with low elevation can be described by the solution of the wave equation $\nabla^2\psi + k^2n^2\psi = 0$, where $\nabla \equiv (\partial/\partial x, \partial/\partial y)$ is the horizontal gradient operator, $k = 2\pi/\lambda$ is the free-space wavenumber, and n is the refractive index. $\psi(x,z) = u(x,z)e^{jkx}$ is the electric field component, and $u(x,z)$ is the envelope function where x and z stand for transverse, i.e., the direction of propagation.

Using the assumptions that the field is a far field, the envelope function $u(x,z)$ changes slowly with angle, and then the standard parabolic equation can be written as:

$$\frac{\partial^2 u}{\partial x^2} + 2jk\frac{\partial u}{\partial z} + k^2(n^2-1)u = 0 \tag{3}$$

The solution in $x-z$ at a range step Δx is given by applying the inverse Fourier transform to the resulting solution.

$$u(x+\Delta x,z)=FFT^{-1}\left[e^{jk\Delta x(\sqrt{1-\frac{p^2}{k^2}}-1)}FFT[u(x,z)]\right]=FFT^{-1}\left[e^{jk\Delta x(\cos\theta-1)}FFT[u(x,z)]\right] \quad (4)$$

where $p=k\sin\theta$, θ is the propagation angle relative to the horizon, i.e., the elevation angle of the satellite in our experiments. Many numerical methods are concerned with obtaining approximate solutions of Equation (4) [10, 11]. In this paper the Fourier split-step method is used [12].

3.2. Simulation

Figure 1(a) shows the geometry of incident GNSS radio wave on the ground and then reflected from the ground to the receiver. Here a soil block with height of h_{block} is placed on the flat ground, and the distance from the block to the receiving antenna is d_{block}. In the later simulation, different values of h_{block} and d_{block} are considered to investigate the effect of terrain on GNSS signals propagation. In the case of $h_{block}\neq 0$ or $d_{block}\neq 0$, the antenna will receive not only the direct signal and the reflected signal from the ground, but also the signal scattered from this soil block.

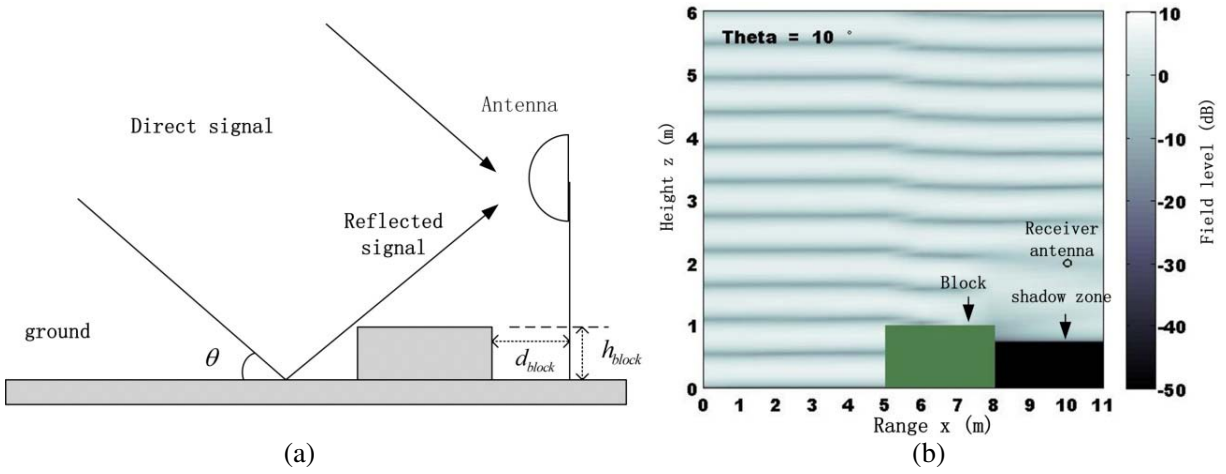

Figure 1. (a) GNSS signals reflected over terrain; (b) Computed field over terrain element (a shadow zone behind the soil block).

In our simulation, the radio frequency is the same as GPS L1 frequency of 1.5 GHz. The total domain range is 11 m, the domain height 6 m, and the soil block width 3 m. The receiving antenna is located at $x=10$ m, $z=2$ m, which is omnidirectional in order to receive the signals from all directions.

Generally for a transmitter with a specified elevation, the PE method calculates and stores field-level values at every range and height point in a two-dimensional field array. As an instance, when the propagation angle is set to 10°, i.e., the GNSS signal of the navigation satellite is incident at an elevation of 10°, the simulated total field in the domain is acquired and shown in Fig. 1(b), where different colors represent different field levels in a two-dimensional field-level array. From the field plot, we can see that the signal strength behind the soil block is decreased due to the shadowing effect of the soil block. In this paper, we focus on the field level at the receiving antenna point when the propagation angle varies from 5°to 30°.

In order to find the relationship between the GNSS satellites elevation (theta θ) and the field level at the receiver antenna point (here the antenna gain is set to 0 dB), the field level at each elevation is calculated. By changing the elevation of transmitter antenna and fixing the receiver point at $x=10$, $z=2$, we get the signal-level values (dB) as a function of elevation.

Three cases are simulated as follows: (1) No terrain block; (2) $h_{block}=0.4$ m, $d_{block}=5$ m; (3) $h_{block}=0.4$ m, $d_{block}=2$ m. In all of these cases, the GNSS signals are reflected from the ground with

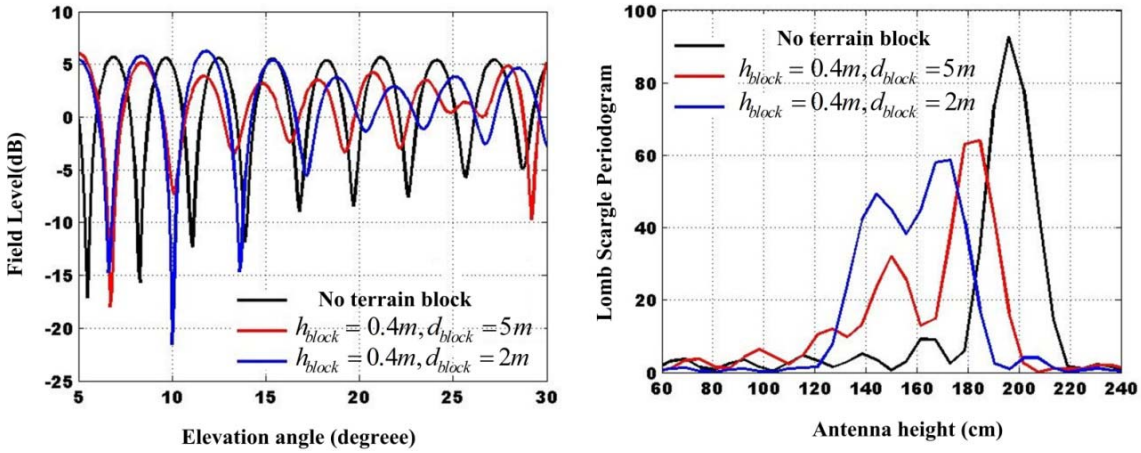

(a) (b)

Figure 2. (a) The interference signals; (b) Corresponding lomb scargle periodograms. In (a) there are phase mutations in red line and blue line. In (b) there are frequency deviations in red and blue line.

dry soil (dielectric constant $\varepsilon = 5$, conductivity $\sigma = 10^{-5}$), and the GNSS elevation changes from 5° to 30° with a step of 0.1°. Some of these cases will occur in the later field experiments.

Figure 2(a) shows the interference signals in these cases. When there is no soil block, the interference signal shows a regular sinusoidal oscillation waveform. However in the case of soil block, phase jumps near 23° (blue) and 25° (red) in the interference signals. Periodograms of the interference signal can be acquired by lomb scargle method [13]. Fig. 2(b) shows the periodograms with obvious frequency deviation and frequency splitting in the cases of soil block, and the block closer to the receiving antenna may cause more severe distortion. The reason is that the terrain block causes more multipath signals than the flat ground, and these multipath signals are received by the omnidirectional antenna.

4. EXPERIMENTS

4.1. Data Processing Steps

Three experiments are conducted to investigate the interference signals over different types of terrains. The block diagram of the data processing to estimate antenna height is shown in Fig. 3, and it involves the following steps:

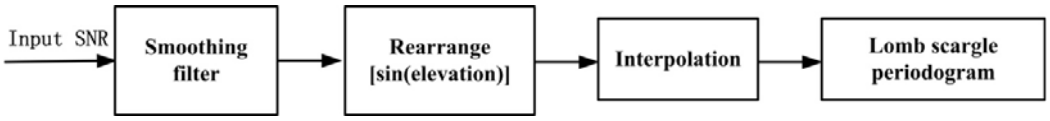

Figure 3. Block diagram of the data processing to estimate antenna height.

1) Obtain the amplitude of the SNR data from the GNSS receiver and choose the data from elevation of 5° to 30°, then filter the data by a smoothing filter to mitigate high frequency noise.

2) Rearrange the data according to the sine of elevation. Since there exist multiple values of the SNR (the resolution of the elevation angle is 1° for our receiver with NMEA0183 format) in every degree, another moving average filter is employed to create an approximating function curve that shows the relationship between the SNR and the sine of elevation.

3) Implement the spline interpolation method to increase the number of data samples to 128 since there are at most 26 samples from 5° to 30°, which are not enough to perform the spectrum analysis.

4) Carry out power spectrum analysis of the data by lomb scargle method. The frequency f of peak power is identified and then translated into the antenna height h according to $f = 2h/\lambda$, where $\lambda = 19.05\,\text{cm}$ for GPS L1 signal and $\lambda = 19.22\,\text{cm}$ for BeiDou system (BDS) B1 signal.

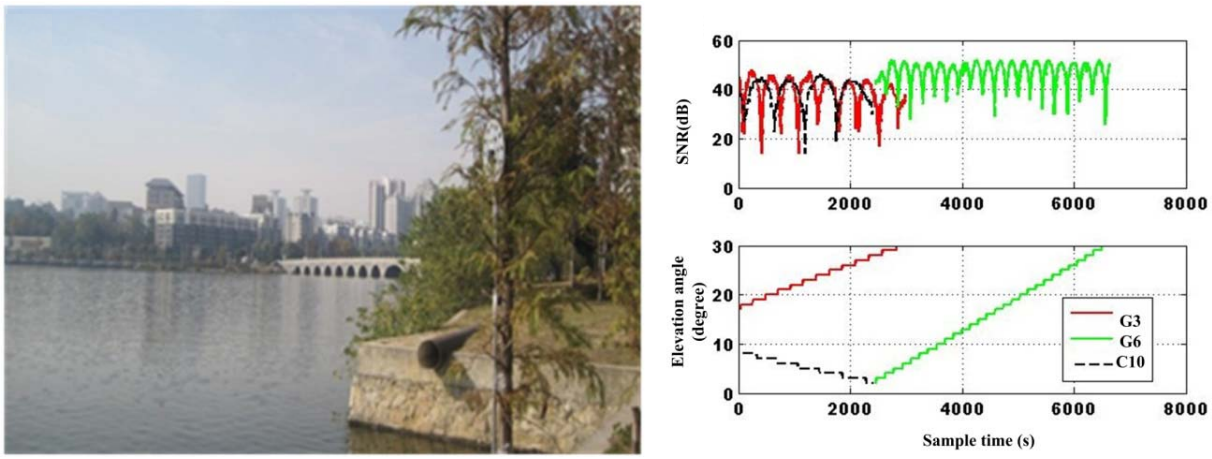

(a) (b)

Figure 4. (a) Horizontal-looking antenna above the water surface; (b) SNR and elevation of satellites C10, G3 and G6.

4.2. Experiment over Water Surface

Our first study is focused on interference signal over water surface. The horizontal-looking antenna is placed at a height of 2 m above the water surface to receive the direct and reflected signals, as shown in Fig. 4(a).

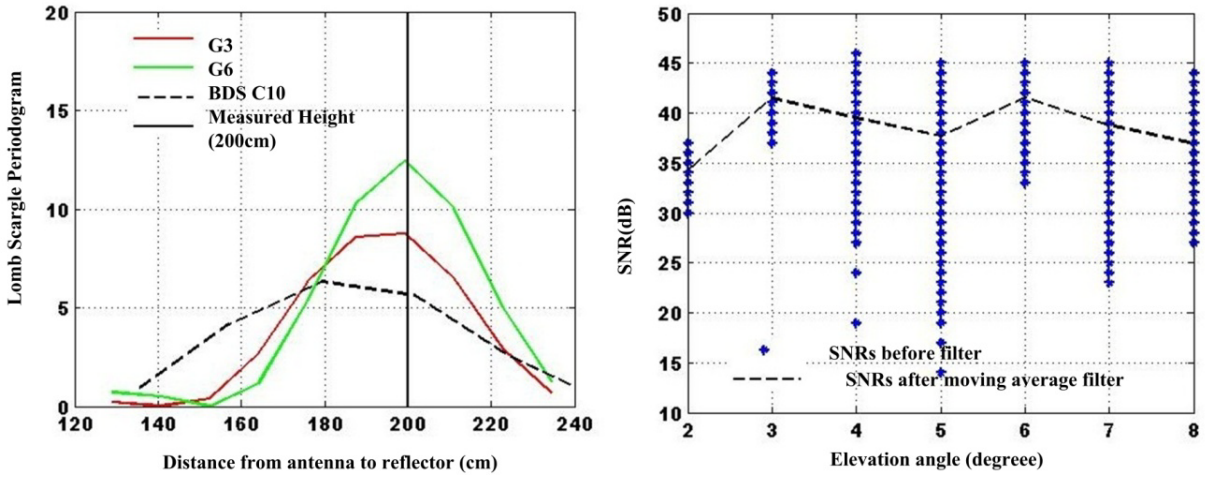

(a) (b)

Figure 5. (a) Lomb scargle periodograms of G3 G6 and C10; (b) The SNR of C10 before and after moving average filter.

Figure 4(b) shows the SNR of G3, G6 and C10 at various sample times. It is visible that SNR change rate $d\theta/dt$ of G6 is faster than that of G3 and C10. However, these satellites have similar height estimation in their periodograms as shown in Fig. 5(a) because the height of the antenna is determined by $d(\sin\theta)/dt$. G3 and G6 give accurate estimation of 200 cm while C10 shows an error of 20 cm for that the number of samples of C10 is finite since the elevation of C10 decreases from 8° to 2° during the experimental time (Fig. 4(b)). Fig. 5(b) shows the SNR of C10 with only 7 samples after smoothing filter.

4.3. Experiment over Ground with Soil Block

The second study is focused on the reflection from ground with soil block. The experiment is conducted in Wuhan University. As shown in Fig. 6, two antennas are placed on a light pole to receive the signals. One is horizontal looking with a height of 190 cm, and the other is zenith looking, which is 10 cm higher than the horizontal-looking antenna.

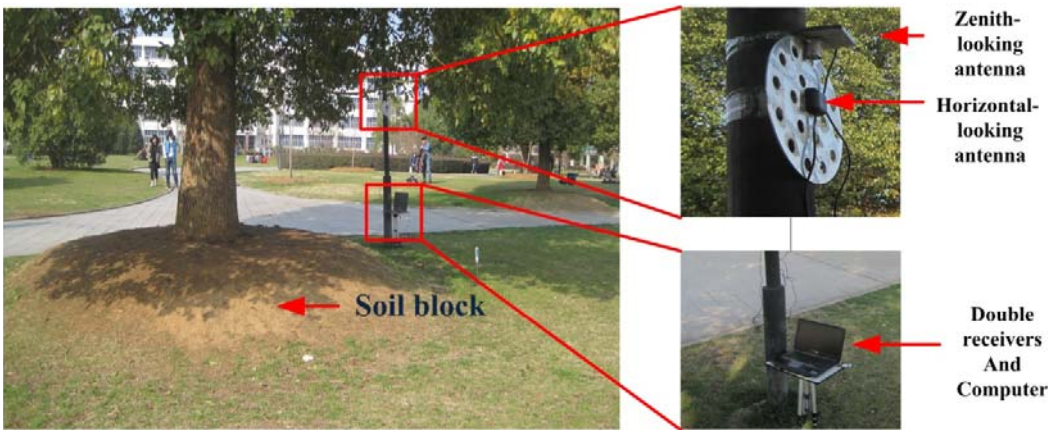

Figure 6. Field experimental with horizontal-looking and zenith-looking antennas and receivers.

The signals received by horizontal-looking antenna are discussed at first. Fig. 7(a) shows the lomb scargle periodograms of the interference signals of C7, G2, G17, G24 and G26, and all of them give correct estimation with error less than 5 cm. However in Fig. 7(b), the lomb scargle periodograms of C8, C10 and G12 give estimation with obvious error. So we check the azimuth of these satellites and find that this phenomenon is caused by the effect of the terrain. At the southwest direction, a soil block about 2 m away from the antenna can be seen in Fig. 6. Since the tracks of C8, C10 and G12 pass through the soil block (see Fig. 8(a)), the soil block leads to serious estimation error as simulated in Section 4.3.

Then the zenith-looking antenna is used to receive the direct and reflected signals to validate this hypothesis that different placements of antenna may suppress the effect of near terrain. Fig. 8(b) shows

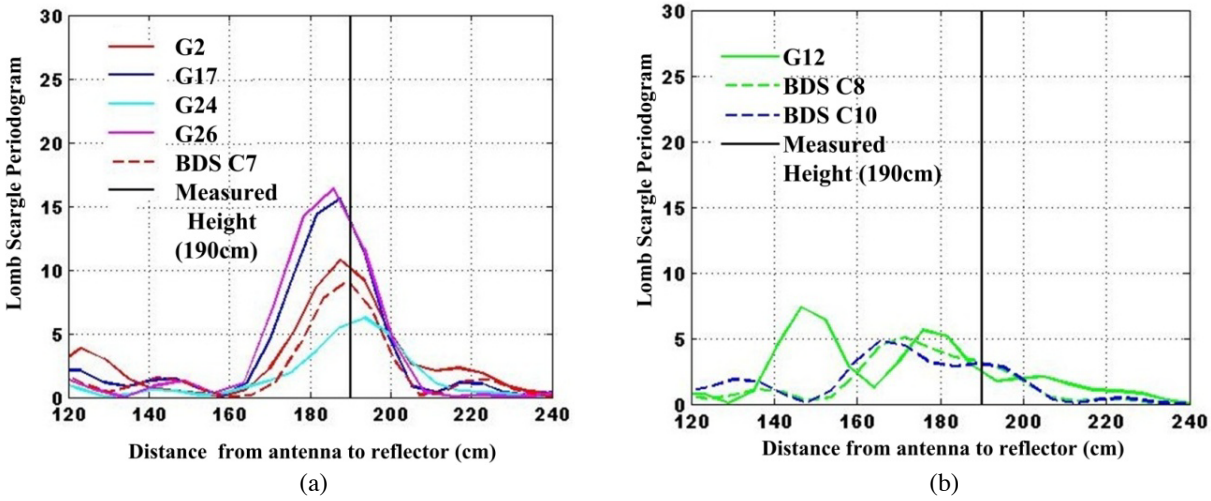

Figure 7. (a) Lomb scargle periodograms of the interference signals of C7, G2, G17, G24 and G26; (b) the lomb scargle periodograms of C8, C10 and G12. All of above signals are received by horizontal-looking antenna.

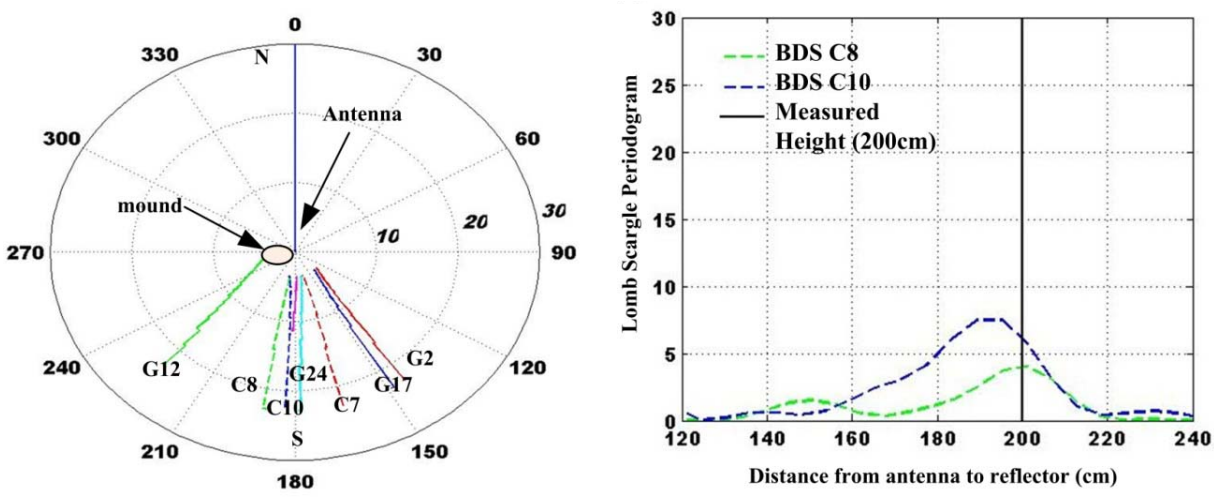

(a) (b)

Figure 8. (a) The reflection point trajectories of eight satellites analyzed in this study; (b) the lomb scargle periodograms of C8 and C10. Signals above are received by zenith-looking antenna.

the lomb scargle periodograms of C8 and C10 (G12 signal is not captured). C8 (green dashed line) gives a correct estimation of antenna height at 200 cm while C10 (blue dashed line) shows an error less than 10 cm. The reason why the zenith-looking antenna can suppress the signals reflected from the near soil block is that microstrip patch antennas are generally designed to suppress signals from the back of the antennas.

4.4. Experiment over Slope Surface

The last experiment is conducted in BaoXie, WuHan, China (longitude: 114.532291°E, latitude: 30.467376°N) which is focused on reflection from slope surface. As shown in Fig. 9, the area around the experimental site is flat. The receiving antenna is fixed to the 2 m high railings above the ground. The front of the railings is an open bare area while the other side is a slope with smooth surface, and its slope is about 55°.

Figure 10 shows the interference signal data of C7 for a whole day. Figs. 10(a), (b) and (c) represent

Figure 9. Experiment site in BaoXie, WuHan, China.

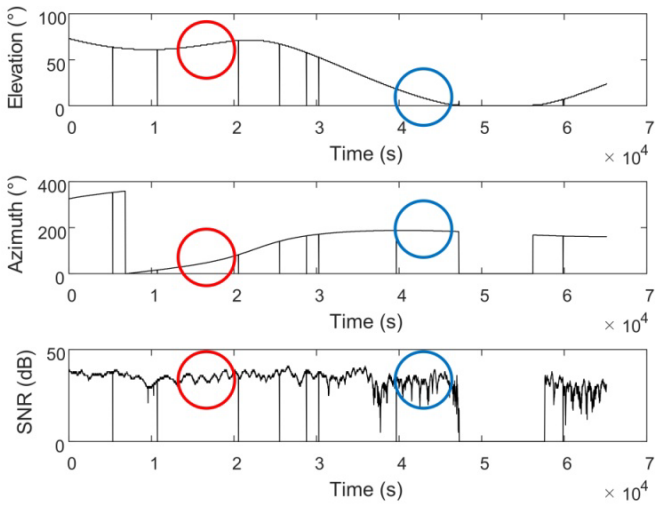

Figure 10. Elevation, azimuth and SNR of C7 in a whole day.

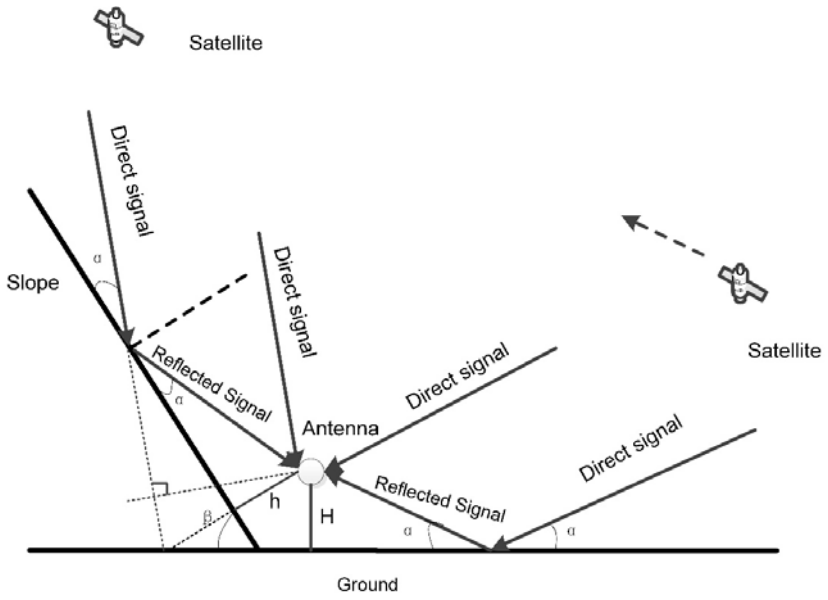

Figure 11. Lateral view of the experimental site.

their elevation, azimuth and SNR, respectively. The SNR manifests a quasi-periodic oscillating pattern in the elevation range of $22 \sim 7°$, and corresponding data segments are marked with a blue circle. In addition, the SNR data of C7 also have another obvious oscillation from elevation of 60° to 70°, which are marked with red circles.

According to the trajectory of C7, the obvious oscillation with high elevation may be due to the signal from the slope surface reflection. A corresponding lateral view of the experimental site is drawn in Fig. 11, which clearly shows the situation that high elevation minus the slope becomes a similar low-elevation. The angle between the slope surface and the ground is β, and the angle between the direct signal and the slope surface is α. The signal reflected from the slope surface enters the antenna. H is the height of the receiving antenna from the ground, while h is the distance from the receiving antenna to the slope surface which can be derived from the f. To verify this assumption, we processed the SNR data of C7 in red circles according to the data processing steps in Section 4.1. There is a difference in step 2 where the elevation subtracts slope before being rearranged. The frequency $f = 30.47\,\text{Hz}$ of

the peak power was obtained, and then the height $h = 2.93\,\text{m}$ was derived from the formula $f = 2h/\lambda$, which is approximately equal to the actual distance between antenna and slop surface 2.75 m.

5. CONCLUSIONS

In this paper, we investigated the effects of terrain and antenna placement on interference signal. We simulated GNSS reflection over ground with a soil block by parabolic equation method and analyzed the interference signal in three cases, including no soil block and soil block with different distances from the antenna. The simulation results show that there is obvious frequency deviation and frequency splitting in the cases of soil block, and the block closer to the receiver antenna may cause more severe distortion. Then we conducted three typical field experiments. The results show that height estimation results of both horizontal and zenith looking antenna are correct when the ground is flat. When the ground is not flat, the soil block near the receiving antenna leads to estimation error. By using zenith-looking antenna to suppress the influence from the near terrain, a more accurate estimation is obtained than using horizontal-looking antenna. When a slop is near the antenna, the signal with a high elevation can achieve an obvious interference effect if high elevation is equivalent to a low elevation after subtracting slop. In this situation, the estimated height is the distance between antenna and slope surface. In the future, we intend to investigate the reflected signals from complex terrain and conduct more experiments to study the remote sensing using GNSS reflected signals.

ACKNOWLEDGMENT

This paper is supported by the National Natural Science Foundation of China under grant 41571420.

REFERENCES

1. Li, W., et al., "First spaceborne phase altimetry over sea ice using TechDemoSat — 1 GNSS — R signals," *Geophysical Research Letters*, Vol. 44, No. 16, 8369–8376, 2017.
2. Han, M., et al., "A semi-empirical SNR model for soil moisture retrieval using GNSS SNR data," *Remote Sensing*, Vol. 10, No. 2, 280, 2018.
3. Yan, Q. and W. Huang, "Sea ice sensing from GNSS-R data using convolutional neural networks," *IEEE Geoscience and Remote Sensing Letters*, Vol. 99, 1–5, 2018.
4. Zhang, S., et al., "Use of reflected GNSS SNR data to retrieve either soil moisture or vegetation height from a wheat crop," *Hydrology and Earth System Sciences*, Vol. 21, No. 9, 4767–4784, 2017.
5. Yan, S., et al., "Feasibility of using signal strength indicator data to estimate soil moisture based on GNSS interference signal analysis," *Remote Sensing Letters*, Vol. 9, No. 1, 61–70, 2018.
6. Rodriguez-Alvarez, N., et al., "Snow thickness monitoring using GNSS measurements," *IEEE Geoscience and Remote Sensing Letters*, Vol. 9, No. 6, 1109–1113, 2012.
7. Arroyo, A. A., et al., "Dual-polarization GNSS-R interference pattern technique for soil moisture mapping," *IEEE Journal of Selected Topics in Applied Earth Observations and Remote Sensing*, Vol. 7, No. 5, 1533–1544, 2014.
8. Zavorotny, V. U., et al., "A physical model for GPS multipath caused by land reflections: Toward bare soil moisture retrievals," *IEEE Journal of Selected Topics in Applied Earth Observations and Remote Sensing*, Vol. 3, No. 1, 100–110, 2010.
9. Hannah, B. M., K. Kubik, and R. A. Walker, "Propagation modelling of GPS signals," *IFP*, 137, 1999.
10. Sevgi, L., C. Uluisik, and F. Akleman, "A matlab-based two-dimensional parabolic equation radiowave propagation package," *IEEE Antennas and Propagation Magazine*, Vol. 47, No. 4, 164–175, 2005.
11. Hannah, B. M., "Modelling and simulation of GPS multipath propagation," 2001.

12. Apaydin, G. and L. Sevgi, "The split-step-fourier and finite-element-based parabolic-equation propagation-prediction tools: Canonical tests, systematic comparisons, and calibration," *IEEE Antennas and Propagation Magazine*, Vol. 52, No. 3, 66–79, 2010.
13. Pardo-Iguzquiza, E. and F. J. Rodríguez-Tovar, "Implemented Lomb-Scargle periodogram: a valuable tool for improving cyclostratigraphic research on unevenly sampled deep-sea stratigraphic sequences," *Geo-Marine Letters*, Vol. 31, Nos. 5–6, 537–545, 2011.